Manganese Peroxy intermediates

Name: Afreen Shaik

Roll No: 20P0490001

Inorganic Chemistry, Part-II

School of Chemical Sciences, Goa University

CERTIFICATE

This is to certify that the dissertation entitled "*Manganese peroxy intermediates*" is bonafied work carried out by Ms. Afreen shaik under my supervision in partial fulfilment of the requirement for the award of the degree ofMaster of Science at School of Chemical Sciences, Goa University.

Dr. Sunder N. Dhuri

Project Guide

Prof. Dr. Vidhyadatta M. S. Verenkar

Dean

School of Chemical science

Goa University

DECLARATION

I hereby declare that embodied in this report entitled “Manganese peroxy intermediates” was carried out by me during the year 2021-2022 under the guidance of Dr. Sunder N. Dhuri. In keeping with the general practices of reporting scientific observations, due to acknowledgements have been made whatever the work described is based on the findings of other invesgators.

.

AFREEN SHAIK

M. Sc Part II, Inorganic Chemistry

School of Chemical Sciences

Goa University

ACKNOWLEGEMENT

The literature review entitled "manganese peroxy intermediates " has been successfully completed under the guidance of Dr. Sunder N. Dhuri during the year 2021-2022 in the partial fulfillment of the requirements for the degree of Master of Science in Chemistry.

I had a good learning experience learning the importance and future prospects of undertaking a literature survey which was possible due to timely guidance of Dr. Sunder N. Dhuri and our respected Dean Prof. Dr. Vidhyadatta Verenkar . I also thank the entire library faculty for helping me out for searching relevant books with respect to my topic.

Last but not the least I thank my parents ,friends and other people who are directly and indirectly in the successful completion of my literature survey.

INDEX

Sr.no.	TITTLE	Page no.
1	Introduction	1-4
2	Literature survey	5-11
a.	Experimental	5
b.	Synthesis	5
c.	Computational studies	9
d.	Reactivity	10
e.	Result	11
3	Conclusions	15
4	References	16-17

INTRODUCTION

The key intermediates formed during the dioxygen activation by various metal -containing enzymes are the metal dioxygen compounds . Due to the different oxidation states manganese plays a vital role in the active sites of several metalloenzymes in redox reactions. Studies on a large number of Mn–peroxo intermediates have provided in-depth knowledge of their molecularand electronic structures and such intrinsic properties have been correlated with the reactivity of active sites of manganese-based enzymes.A mononuclear manganese(III)–peroxo complex $[MnIII(N_3Py_2)(O_2)]^+$bearing a non-hemeligand was synthesized by the reaction of $[Mn(N_3Py_2)(H_2O)](ClO_4)_2$ with hydrogen peroxide and triethylamine in CH_3CN at 25 °C[1].It is difficult to study coordination environments around metal centers in biological macromolecules due to the fact that they make up only a small portion of the overall structure.[2]

Lipoxygenase-catalyzed dioxygenation of polyunsaturated fatty acids leads to the formation of reactive fatty acid hydroperoxides.[3]

Manganese is the common transition metal in the natural environment. Aqueous Mn (II) is generally regarded as an inefficient trigger for persulphate activation.Manganese intermediates might be invoked in Mn (II)/persulfate conjugations for decontamination.[4]Manganese complexes are widely used as oxidation catalystbased on their rich redox chemistry, however the use of complexes of transition metals in industrial processes is limited by its low catalytic actions[5].The ligand structure are based on N- hydroxylethylethylenodiamine group with pyridine or phenolic arms[5].

Many of the Mn-peroxo species reported in the literature have been observed as primary ions in mass spectrometric (MS) characterization of synthetic products . MS alone cannot provide detailed structural information so ion structures canbe obtained through theoretical analysis of the sharp vibrational spectra available when MS is coupled with spectroscopic probes such as cryogenic ion vibrational predissociation (CIVP) spectroscopy[6].

Here we demonstrate the efficacy of the CIVP method for analyzing dioxygen compounds by identifying the O - O stretching fundamental in the $[Mn(tmc)O_2]^+$.[7]

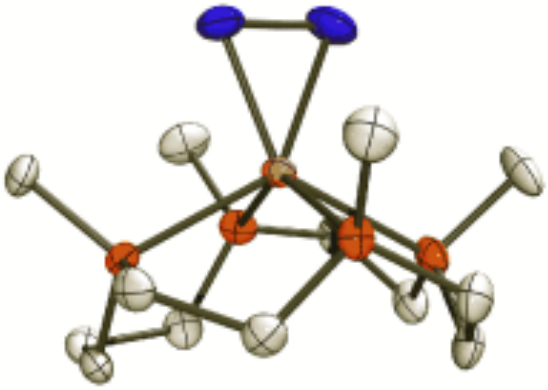

$[Mn^{III}(13\text{-}TMC)(O_2)]^+$ (1)

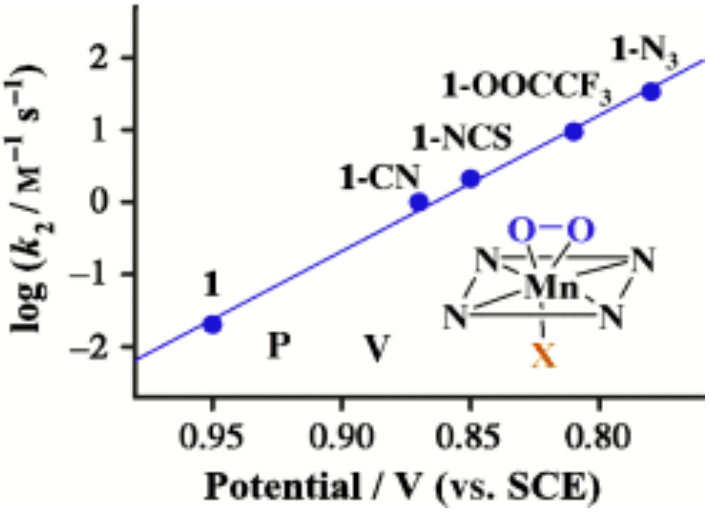

Table 1

Measured $\nu_{o\text{-}o}$ frequencies (cm−1) in this work and other "side-on" Mn-peroxo species compared to the analogous O- O bond lengths (Å)obtained via X-ray crystallography.

Species Phase	Phase	$\nu_{O\text{-}O}$ frequency (cm−1)	O-O A^O
$Mn^{III}(TPP)O_2$	Air matrix	983	1.421
$[Mn^{III}(tmc)O_2]^+$	Gas	970±6	1.403
$Tp^{iPr}2Mn^{III}(\eta^2{-}O_2)(im^{Me}H)$	Solid(KBr)	896	1.42
$Mn^{III}(O_2)(3,5\text{-}iPr_2pzH)(HB(3,5\text{-}iPr_2pz)_3)$	Solid(KBr)	892	1.428
$[Mn^{III}(S^{Me2}N_4(QuinoEn))(OOtBu)](BPh4)$	Solid(NaCl)	888	1.457
$[Mn^{III}(O_2)H_2bupa]{-}$	solution	885	N/A

Structural characterization of metal centers capable of binding and activating O_2 are of interest both to natural and synthetic catalysis . For example, Mn-peroxo complexes are involved in the mechanisms of Mn catalase and superoxidedismutase reactions, and could even be at play in photosystem II . Considerable effort has been directed toward synthesis and characterization of Mn-peroxo complexes, their structural properties have proven difficult to obtain with traditional methods of analysis (e.g.,X-ray,UV–vis,etc.)

.For example ,while EPR and electronic absorption spectroscopies areroutinely used to deduce the overall spin and the electronic state of Mn(III)O_2 complexes, these methods yield only indirect information about their geometries . The most detailed structural information comes from X-ray structuresWhen the peroxo species are sufficiently stable to be crystallized , where O_2 has been shown to bind directly to the metal center in a side-on fashion with O - O bond lengths ranging from 1.40 to 1.43 ˚ A .

Relatively stable peroxocompounds can also be characterized using infrared and Raman spectroscopy[7].

Millions of tons of high-value oxygenated compounds are annually produced and applied to the manufacturing of fine chemicals worldwide ,catalytic oxidations are core processes in petrochemistry. In nature, the ubiquitous cytochrome P450 enzymes (P450s) with an iron protoporphyrin IX core catalyze a wide variety of oxidation reactions with exceptionally high reactivity and selectivity . Many transition metal complexes are designed to develop bioinspired oxidation catalysts and to aid in understanding important biological processes . As a result, these synthetic catalysts typically consist of transition metals such as iron, manganese, chromium [7].Understanding the redox cycling of metal ions in natural and biomimetic systems for dioxygen activationin catalytic oxidation processes at the molecular level has stood at the center of interest for many years [8].

Heme- and non-heme-containing metal complexes have long attracted interest . Their contributions to the understanding of the enzyme mechanisms of, for example, cytochromes P-450 and insights into mechanisms of oxygenation that are useful in industry. The definitive experiments establishing these metal-oxo species as the reactive intermediates include the use of isotopically labeled water, $H_2{}^{18}O$, and involve two sequential reactions. In the first reaction, the ^{18}O label confirmed the equilibration of the metal-oxo moiety with the labeled water, $H_2{}^{18}O$, to form the labeled catalyst intermediate LMd^{18}O (L) porphyrin. In the second step, the labeled metal complex LMd^{18}O was identified as the source of the oxygen atom that is transferred to the olefin, thereby supporting the oxygen rebound mechanism iates for catalytic epoxidations mediated by iron, manganese, and chromium porphyrin.

Recent investigations in these laboratories have shown that the hydrogen peroxide adduct of the oxidized manganese complex can transfer an oxygen atom directly to the substrate from the peroxide molecule by a Lewis acid pathway, rather than involving a redox change at the metal atom[9].

Thiocarbonyl compounds such as substituted-thioureas, -thioamidesfound to react with a peroxysulfur intermediate[10].Lignin is a complex heterogeneous and random phenyl propanoid polymer that constitutes 20-30% of woody plants.Different works have reported the predominance of hydroxylated products that disappears at the end of the treatment with a decrease in toxicity, as well as polymerization occurrence after degradation of the parent compound .

Conversely, the identification and evaluation of TPs and their toxicity requires a more in-depth approach to expand the results to emphasize the applicability of enzyme degradation treatments[11].

homoprotocatechuate 2,3-dioxygenases enzyme exhibit 83% sequence identity, yet their activities depend on different transition metals, Mn_2 and Fe_2[12].

Lignin is a complex heterogeneous and random phenyl propanoid polymer that constitutes 20-30% of woody plants[13] Since the biodegradation of cellulose is retarded by the presence of lignin, the catabolism and utilization of this polymer are of enormous significance (2-5). White rot basidiomycetous fungi are primarily responsible for the initial decomposition of lignin in wood .When cultured under ligninolytic conditions the white rot basidiomycete Phanerochuetechrysosporium produces two heme peroxidases which along with an H_20_2 generating system appear to be the major components of its lignin degradative system . Electronic absorption , EPR, and resonance Ra- man spectral evidence indicates that the heme environment of native MnP has features which are similar to those of other plant peroxidases[14].

Recently, manganese(III) acetate has been widely used for the carbon-carbon bond formation in organic synthesis[15].

A central challenge in modern chemical synthesis is to replace economically and environmentally unsustainable and energy demanding methods.Manganese, together with iron has proven to be one of the more promising metals on which to base new catalytic oxidation systems. In the case of manganese, this is in large part due to the remarkably versatile redox chemistry of manganese with the formal oxidation states II–V and VII being readily accessible. MnIII and MnIV mono- and multi-nuclear complexes are kinetically much more stable with regard to ligand exchange and exhibit, generally, quite intense UV absorption bands, assigned to ligand to metal charge transfer transitions, and moderately intense visible and near-infrared absorption bands, the latter bands generally being assigned to metal centred transitions[16].

Oxidation of phenols by molecular oxygen catalysed by cobalt(II) or manganese(III) complexes represents a typical example of a reaction involving the activation of dioxygen by a transition metal cation. These reactions, known since 1967, have been the subject of numerous studies which have aimed either at optimising the experimental conditions, or at finding more efficient catalysts, or at obtaining a better knowledge of their mechanism and in particular of the role played by the metal ion.[17]

rate of reaction is first order in [Mn(III)] and independent of both [Mn(II)] and [H_20_2] concentrations[18].

Organic peroxides are a class of valuable compounds, which have gained appreciable attention in pharmaceutical science, biological chemistry and food chemistry. Besides, peroxides also act as effective radical initiators, powerful oxidants and key reactive intermediates in synthetic chemistry.[19]

In biomimetic studies, a number of metal–O_2 adducts have been synthesized and characterized with various spectroscopic methods, and their reactivities in the oxidation of organic substrates have been extensively investigated. Complexes are also invoked as reactive intermediates in the reactions of Mn-containing enzymes, such as manganese superoxide dismutase, catalase, and the oxygen-evolving complex of photosystem(II). In biomimetic studies, a number of Mn–peroxido complexes have been synthesized and characterized with a variety of spectroscopic methods including X-ray crystallography. A notable example is the first X-ray crystal structure of a side-on peroxido manganese(III) porphyrin complex ([MnIII(tpp)(O_2)]. [20]

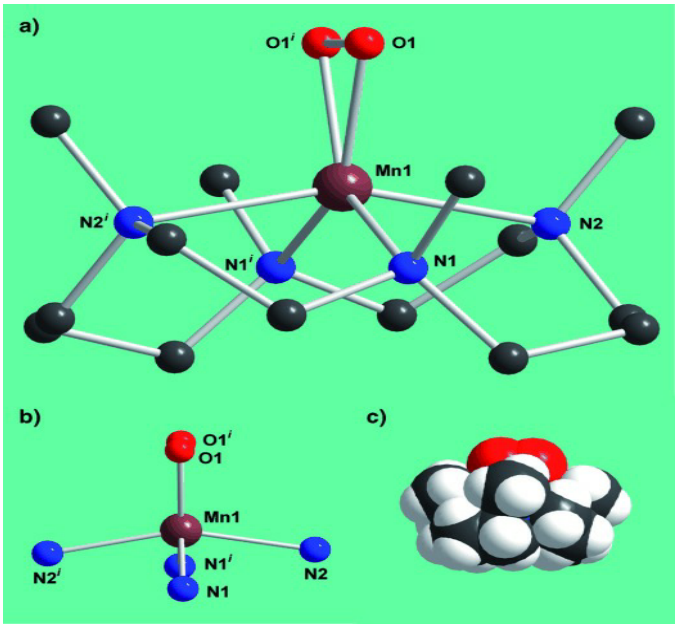

Structure of [MnIII(tmc)(O2)]+ (1). b) View of the distorted octahedral Mn(N4O2) moiety. c) Side view (space-filling representation) derived from the crystal structure determination.

Peroxidomanganese(III) complexes are also invoked as reactive intermediates in the reactions of Mn-containing enzymes, such as manganese superoxide dismutase, catalase, and the oxygen-evolving complex of photosystem II[21].

LITERATURE REVIEW

Experimental

SYNTHESIS :

1] [MnIII(N_3Py_2)(O2)]$^+$ {Manganese(III)–peroxo complex}]

All solid chemicals used in this work were used as received without recrystallization. Before using the solvents were dried and distilled under a N_2 atmosphere . N_3Py_2 and [Mn(N_3Py_2)(H_2O)](ClO_4)$_2$ were prepared according to recent reports

A dry powder of sodium hydride (0.3 g) was taken in DMSO-d_6 maintained under an Ar atmosphere, and then the temperature was brought down to 0 °C . 2-Phenyl propionaldehyde (2-PPA) (1.335 mL) was then slowly added (it is an exothermic reaction) and the temperature of the reaction mixture was then slowly increased to 25 °C. The solution was kept for 8 h under stirring and then neutralization was done with D_2O, followed by extraction with ethyl acetate. By ^{1}H NMR spectroscopy Purity of >99% deuteration in the product was confirmed. ^{1}H NMR spectra were measured with a Bruker model Ascend 400 FT-NMR spectrometer.[4]

2. $[Mn(N_3Py_2)(H_2O)](ClO_4)_2]$

N_3Py_2 (0.452 g, 1.38 mmol) in CH_3CN (2 mL) was added to Mn $(ClO_4)_2 \cdot 6H_2O$ (0.5 g, 1.38 mmol) (2 mL CH_3CN) at RT under a N_2 atmosphere. A brown solution was obtained by stirring the reaction mixture for 12 hr. A white-buff powder was formed by addition of diethyl ether which on work-up gave yield = 0.68 (82%). Calculation for $C_{19}H_{31}N_5Cl_2O_9$

Mn: C, 38.08; H, 4.91; N, 11.69%. Found C, 38.19; H, 4.91; N, 11.59%. IR (KBr, cm−1): 3412 ν(O–H); 1093, 621 ν(ClO4). Magnetic moment, μeff = 5.97 BM. ESI-MS: m/z = 191.18 (Calc. m/z = 191.21): $[Mn(N_3Py_2)]^{2+}$ and m/z = 481.08 (Calc. m/z = 481.86): $[Mn(N_3Py_2)(ClO_4)]+$[4].

3. Diperchlorate of aqua(N,N,N^I-tris(2-methylpyridyl)-N^{I}hydroxiethyl-ethylenediamine manganese(II),

$[MnL1(H_2O)](ClO_4)_2]$

N,N,N-tris(2-methylpyridyl)-N^{1}hydroxyethyl-ethylenodiamine, (L1)

$Mn(ClO_4)_2 \cdot 6H_2O$ (5.42 g, 1.50 mmol), $NaClO_4 \cdot H_2O$ (0.51 g,4.17 mmol) and L1 (6.08 g, 1.61 mmol) were dissolved in 40 mL of anhydrous ethanol and kept under reflux at 40◦C for 1 h. Aftercooling to room temperature and slow addition of diethyl ether,a light yellow powder precipitated. It was then washed with coldwater and dried under vacuum.

Suitable crystals for X ray diffraction analysis were obtained by slow diffusion of diethyl ether to anacetonitrile solution of the complex. The yield was 4.68 g (48.05%).Elemental analysis for $C_{22}H_{29}N_5Cl_2O_{10}Mn$: (649.34 g mol−1) calcd. C, 40.69; H, 4.50; N, 10.79%; found C, 40.70; H, 4.50; N, 10.80%.

4. Perchlorate Of N-(2hydroxibenzyl) N,N^I - bis(2-methylpyridyl) – N^{I}hydroxiethyl ethylenodiaminemanganese(II) ,

$[MnL_2]ClO_4$

N-(2-hydroxibenzyl)-N,N^{I}-bis(2-methylpyridyl)-N^{I}-hydroxiethyl-ethylenodiamine, (L2)

Trethylamine (3.5 mL, 25 mmol) and 5.94 g (15.1 mmol) Of L2 were dissolved in anhydrous ethanol at 65°C for 5 min.Then, $Mn(ClO_4)_2 \cdot 6H_2O$ (5.43 g, 15.0 mmol) and NaClO4·H2O (0.42 g,3.43 mmol) were added and the solution was refluxed for 1 h. A brown solid was separated by filtration, washed with cold water ethanol, ether and dried under vacuum. The yield was 4.3 g (52.6%).Suitable crystals for X ray diffraction analysis were obtained asdescribed for $[MnL2]ClO_4$. Elemental analysis for $C_{23}H_{27}N_4ClO_6Mn$:(544.87 g mol−1) calcd. C, 50.51; H, 5.01; N, 10.68%; found C, 50.42;H, 5.33; N, 10.23%. [5]

Batch experiments were initiated by adding persulfates (i.e., PMS or PDS) into pH-adjusted solution containing target contaminants, Mn(II), with and without complexing ligand at desirable concentrations.At proper time intervals, reaction solution was sampled and quenched by excess ascorbic acid before analysis with high pressure liquid chromatography (HPLC) and UV detection. In parallel, another sample was withdrawn for spectrophotometric measurement of persulfates concentration . Preliminary experiments demonstrated that the initiating way (adding persulfates immediately into solutions versus 1 hour later) had no influence on the reactions. Control experiments without addition of persulfates or Mn(II) were also conducted under identical conditions. Reactions involving Mn(III) were initiated by adding target contaminants or simultaneously adding persulfates and target contaminants into prepared Mn(III) solutions. Acetate sodium (10 mM) was used as buffers for pH 5 and borate sodium (10 mM) was used as buffers for pH 8. The changes of solution pH were less than 0.2 units during the reactions. All the experiments were performed at least in duplicates at 25 °C and average data were presented. The relative standard deviations were always < 10% unless otherwise stated. For the identification of the molecular ion mass change during Mn(II)/ligand/PMS system, the resulting solution was analyzed by electrospray ionization-triple quadrupole mass spectrometry (ESI −MS). Control experiments for the analysis of solutions containing Mn(II) and EDTA As well as Mn(III)-EDTA were also conducted.[5]

CIVP spectroscopy is an action method that yields vibrational spectra analogous to those commonly obtained with FT-IR instruments, but does so on ions extracted from the same ion sources widely used for high resolution mass spectrometry . The infrared spectra are often much simpler than those obtained with FT-IR because CIVP necessarily interrogates ions that are held at low temperature[6]. The overall scheme involves extraction of the ions from a millimolar solution into the gas-phase with an electrospray ionization (ESI) interface, guiding them through differential pumping stages with RF-ion guides into a 90◦ DC turning quadrupole , and injecting them into a 30K cryogenic ion trap. Once in the trap, ions are cooled .Isotopologuesof$[MnIII(tmc)O_2]^+$, respectively. Though higher volume percentages of N_2 gave larger abundances of the N_2 adduct ions, it greatly decreased signal stability due to condensation of the buffer gas onto the ion trap.

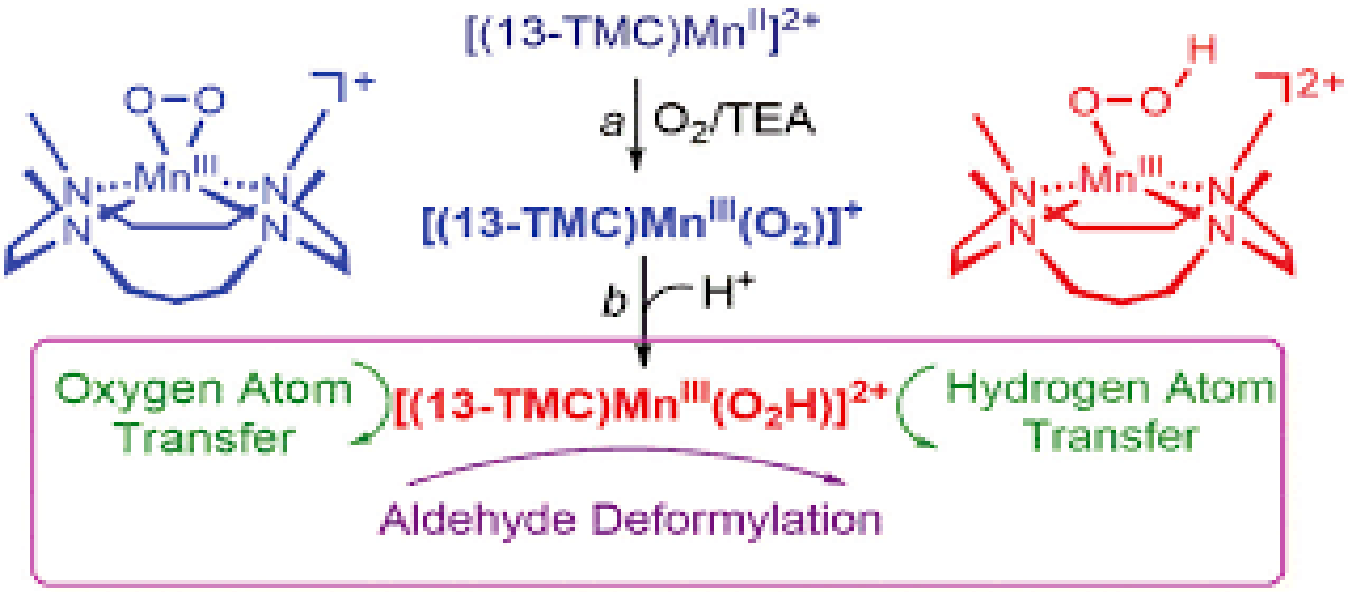

ESI Mass Spectrometry. An acetone solution of 20 mM Mn(Me2EBC)Cl2 was first treated with 2 equiv of AgPF6 to remove chloride. The resulting solution (1 mL) was mixed with excess 70% TBHP to initiate the oxidation, and the reaction mixture was examined by the ESI mass spectrometer in minutes. Skipping the removal of chloride prior to TBHP addition produced a weaker signal attributable to Mn(Me2EBC)(O)(t-OOBu)+. The mass spectrometer used in these experiments is the instrument identified at the beginning of the Experimental Section[9].

Reagents were purchased the stock solution contains IMB in methanol to an initial concentration of 12 g L-1. The working solutions were prepared with the aqueous matrices (DW and SW) by diluting the stock solution until obtaining a final concentration of 1 mg L− 1 of IMB (initial concentration for the degradation assays).

Enzymatic reactions were carried out in succinic/lactic acid buffer (100 mmol L-1) pH 4.5 containing 1 mg L-1 of IMB. Reactions were performed at 50ºC with varying the initial concentrations of MnP (from 0.25 to 2 U L-1), H2O2 (from 0.01 to 3 mmol L-1), and $Mn2^{+}$(from 0.01 to 1.5 mmol L-1). For the optimization step, the reaction vials (2 mL) were stirred on a gyratory shaker (200 rpm) for 4 h[11].

The experiments using the optimal conditions were performed in a batch configuration with a total working volume of 50 mL. The pH value of 4.5 was selected due to a greater stability of the enzyme at this pH, according to different degradation studies , which confirm that a value between 4 and 5 is the most conducive to working with the enzyme. Quantitative analysis of IMB during the optimization step was performed by Waters e2695 HPLC-PAD chromatography system. Before analysis in the HPLC-PAD, the samples were filtered using a 0.45 µm cellulose acetate syringe filter.

In all kinetic measurements, fresh solutions of the manganese complex were prepared by dissolving the appropriate weight in the minimum amount of hydrochloric acid. The pH was then adjusted to the desired value by the addition of ammonia buffer. Sodium nitrate was added to maintain the ionic strength at 0.10 M unless otherwise specified. The mixture was thermostated in a controlled temperature bath and the kinetic run was started by injecting the peroxide into the solution. Samples of the reaction mixture were removed at set time intervals and the reaction was quenched by KI/H,SO, mixture. The liberated iodine equivalent to the residual peroxide contents was then determined iodometrically[18].

Computational studies

The experimental characterization gave a formula of $[Mn(N_3Py_2)(^{16}O_2)]^+$ as [Mn(N3Py2)(η2-O2)]+. However, two isomeric structures for $[Mn(N_3Py_2)(^{16}O_2)]^+$ are possible

1. end-on $[Mn(N3Py2)(\eta1\text{-}O2)]^+$
2. side-on $[Mn(N3Py2)(\eta2\text{-}O2)]^+$

End-on $[Mn(N_3Py_2)(\eta1\text{-}O_2)]^+$. All the possible spin states of the end-on $[Mn(N_3Py_2)(\eta1\text{-}O_2)]^+$ species are optimized using the B3LYP-D2 functional. Our DFT calculations reveal that the quintet state (high spin) is computed as the ground state, and this is consistent with the earlier reports on similar ligand architectures. The triplet state lies at 107.6 kJ mol−1 higher in energy, while a low-spin singlet lies at 164.4 kJ mol^{-1} higher in energy.

Side-on $[Mn(N_3Py_2)(\eta2\text{-}O_2)]^+$. The possible spin states of the side-on $[Mn(N_3Py_2)(\eta2\text{-}O_2)]^+$ species are also optimized. The B3LYP-D2 computed results show that the triplet and the singlet lie at 99.6 and 152.6 kJ mol−1, respectively. The optimized structure of the side-on $[Mn(N_3Py_2)(\eta2\text{-}O_2)]^+$

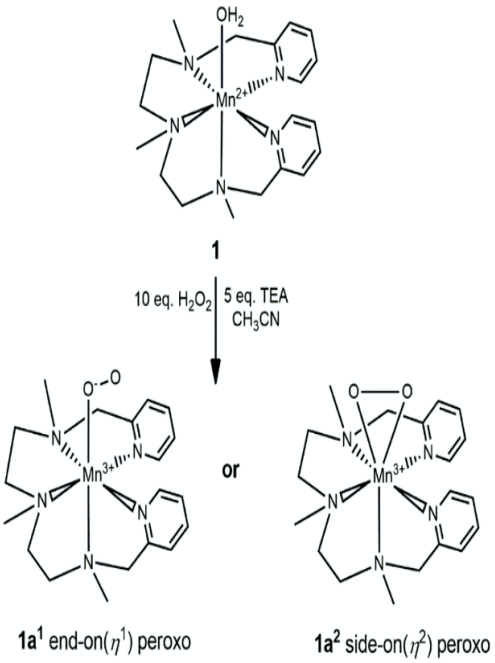

Probable structure of the reactive intermediate Mn(III)–peroxo intermediate which can exist as side-on (η2) or end-on (η1) peroxo

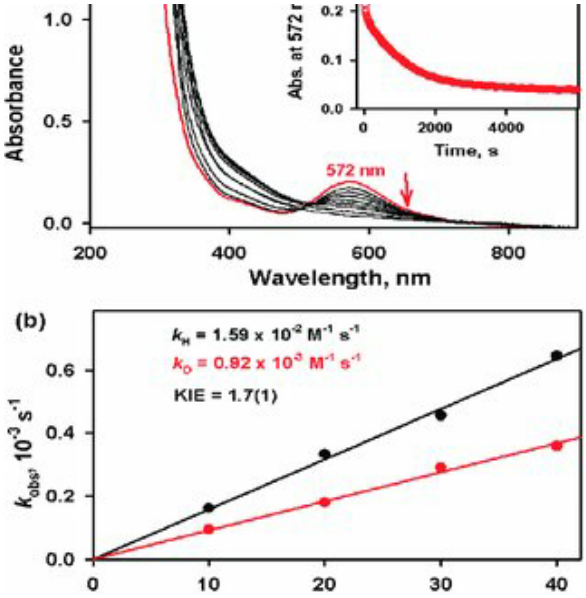

(a) UV-visible spectral changes of 1a (1 mM) upon addition of 10 equiv. of 2-PPA in acetonitrile. The inset shows the time course of the reaction monitored at 572 nm. (b) A plot of kobs against the concentration of 2-PPA and 2-PPA-d to determine the second-order rate constant.

Reactivity

Reactivity of $[Mn(N_3Py_2)(^{16}O_2)]^+$ in aldehyde deformylation

The reactivity of $[Mn(N_3Py_2)(^{16}O_2)]^+$ was then investigated in aldehyde deformylation as the precedent study of first-row transition metal–peroxo species showed the reactivity of Mn(III)–peroxo species with aldehydes. Upon addition of 10 equiv. of 2-PPA to the solution of $[Mn(N_3Py_2)(^{16}O_2)]^+$, the UV-visible band at 572 nm decayed with a pseudo-first-order rate constant, $k_{obs} = 1.6 \times 10{-}3\ s^{-1}$, and showed the isosbestic points at 501 and 778 nm[4].

Results

The formation of $[Mn(N_3Py_2)(^{16}O_2)]^+$ intermediate in CH_3CN was monitored by UV-visible spectroscopy. The UV-Vis spectrum of $[Mn(N_3Py_2)(H_2O)](ClO_4)_2$ in CH_3CN exhibits bands only in the UV region which are associated with intra-ligand transitions. The absorption spectrum of $[Mn(N_3Py_2)(H_2O)](ClO_4)_2$ in CH3CN does not show any band in the visible region, which is the typical characteristic feature of high spin Mn(II) centers due to spin forbidden d–d transitions as observed in similar Mn(II) complexes[4]. On addition of 10 equiv. of H_2O_2 to the 1 mM solution of $[Mn(N_3Py_2)(H_2O)](ClO_4)_2$ in CH_3CN in the presence of 5 equiv. of triethylamine (TEA) at 25 °C, the formation of a purple-colored intermediate $[Mn(N_3Py_2)(^{16}O_2)]^+$ was observed with the appearance of a new band at 572 nm.

The harmonic vibrational spectra of the two isomers (side-on and end-on) of the $[Mn(tmc)O_2]^+$ compound were recorded :both calculated spectra are shifted by $24cm^{-1}$ toward higher energy to emphasize the fact that almost all features in the experimental spectrum are recovered remarkably well, including the intensity profiles, where the calculated intensities (km/mol) were divided by the harmonic frequencies to simulate the experimental action spectra[6]. . The patterns of calculated bands associated with the ligand scaffold are quite similar for both isomers. These active ligand modes involve the C - C and C - N stretches in the 700–$1150cm^{-1}$ range and the C - H bends from 1400 to $1525cm^{-1}$.

Manganese(II) complexes of L1 and L2 were prepared by themixture with equimolar amounts of $Mn(ClO_4)_2·6H_2O$ in ethyl alcohol to yield 48% of $[MnL1(H_2O)](ClO_4)_2$ and 53% of $[MnL2]ClO_4$.Preparation of $[MnL2]ClO_4$ required triethylamine to deprotonatethe phenol[6] The positive charges of the complexes were counterbalanced by the perchlorate anion as indicated by the intensestretching mode at 1100 cm−1. The compounds are fairly stable.Complexes With ligands L1 and L2 afforded suitable single crystalsfor structure determinations.In order to help elucidate the composition of the complexes, molar conductance measurements were carried out fromacetonitrile solutions at 298 K. Complexes $[MnL1(H_2O)](ClO_4)_2$and $[MnL_2]ClO_4$ showed conductivities values of 301 and143 S cm2 mol^{-1}, respectively at 298 K, as expected for a 1:2 and1:1 electrolytes

Important role of Mn(III) species To examine whether Mn(III) play an important role, the effect of Mn(III) ex-situ prepared on the reactions of PMS with NP was investigated. It was found that NP was rapidly degraded in the Mn(III)-EDTA/PMS and Mn(III)-NTA/PMS system, accompanied with PMS decomposition[5]. . These finding indicated that a rapid interaction occurred between Mn(III) complex and PMS, resulting in the formation of reactive intermediates, which contributed to NP oxidation. In the Mn(II)/EDTA/PMS system, Mn(III)-EDTA gradually accumulated to its maximum within ~30 min, coinciding with the following rapid stage of NP degradation and PMS decomposition .

Given the sluggish reactivity of Mn(III)-EDTA toward NP, negligible degradation of NP was expected in the initial lag stage, consistent with the observed experimental findings. Comparatively, autocatalysis was not observed in the Mn(II)/NTA/PMS system, where Mn(III) species was rapidly generated within 1 min. In the Mn(II)/PPP/PMS system, Mn(III) species was hardly generated, hindering the subsequent formation of reactive intermediate and no degradation of NP was observed therein. Therefore, it was not difficult to understand the difference of ligands in activating PMS by Mn(II). These findings confirmed that the formation of Mn(III) species was a critical step in the Mn(II)/ligand/PMS system.

Direct reaction between substrates such as norbornylene, styrene, and cis-stilbene and either the manganese(III) or the manganese(IV) complex does not occur in solution even after the mixture is left standing for days at room temperature. Under these conditions, no norbornylene is consumed, and no epoxide can be detected.[9] . Clearly the MnIV complex alone is not capable of epoxidation of norbornylene even though substantial amounts of $[MnIV(Me2EBC)(OH)_2]^{2+}$, whose pKa is 6.86, would be expected to exist as the oxo complex $[MnIV(Me2EBC)(O)OH]^{+}$. Because the manganese(IV) complex is unstable in base, slowly degrading to MnIII(Me2EBC) species, a disproportionation mechanism for decompostion was suspected. The erstwhile Mn(V) complex might well be unstable and decompose spontaneously.

As stated earlier, MnVdO3c (and in a few cases MnIVd O) is frequently proposed to be the active intermediate for epoxidation, and several MnVdO complexes have been isolated from solution and characterized, with the disappointing result that these particular manganese(V) complexes are inactive for direct oxygen transfer from manganese(V)d O to olefins. We have shown that $[MnIV(Me2EBC)(OH)_2]^{2+}$ does not epoxidize olefins, for example, norbornylene. The possibility still exists that a MnVdO derivative, produced by disproportionation in basic solution, might reveal its presence by epoxidation of a substrate. We suggest that the presence or absence of manganese(V) should be distinguished by experiments designed to produce the epoxidation of norbornylene by the manganese(V) formed during disproportionation of Mn(IV) in basic media. Those experiments were conducted: no epoxide product could be detected, and no conversion of norbornylene was observed upon dissolution of the manganese(IV) complex in basic solution in the presence of norbornylene. Further, treatment of the Mn(II), Mn(III) or Mn(IV) complexes with various oxidants, such as PhIO, H_2O_2, and t-BuOOH, in aqueous solution, failed to provide evidence supporting the existence of MnVdO species. In fact, $[MnIV(Me2EBC)(OH)_2]^{2+}$ has been confirmed to be the dominant species by UV-vis spectroscopy. In this context, it should be recalled that the synthesis of $[MnIV(Me2EBC)(OH)_2](PF_6)_2$ was performed by oxidation of $MnII(Me2EBC)Cl_2$ with aqueous H_2O_2.

The presence in the main ligand of π-systems that transmit electron density to the MnVdO moiety, as in the cases of porphyrins and salen ligands, may be necessary to stabilize those MnVdO species. From that perspective, it is not surprising that stable MnVdO species do not exist with these bridged cyclam ligands since they contain only tertiary nitrogen donors and no π-electron systems except for the hydroxo and oxo ligands.

The degradation of IMB in distilled water and simulated wastewater was carried out using the optimal conditions specified in the previous section. The reaction was monitored for 8h and reaction blanks such as (H2O2 – Mn2+ in absence of enzyme) were also evaluated to determine the stability of the pharmaceutical solution at 50 ◦C About 65% and 34% of the initial IMB was removed during the first 4h of reaction in DW and SW, respectively . Moreover, the concentration of IMB in DW did not have considerable changes after the first 4–8h of incubation (68 ± 4). A control sample to test the stability of IMB with temperature, the catalytic action of the enzyme, and effect of $Mn_2^+ + H_2O_2$ on the process showed degradation percentages of 10%, 23%, and 34% respectively throughout the entire experiment proving that the removal of IMB was largely due to the interaction of the enzyme and its cofactors. The high percentage of IMB degradation in DW could be due to prolonged ferric oxidation state of MnP and direct reaction with H_2O_2 in the treatment to form the peroxy ferric complex, which undergoes an internal redox process to produce ferryl radicals state (FeIV=O R•) (reaction 4) .These strong oxidants can oxidize various substrates in two consecutive one-electron transfer reactions (reaction 5 and 6). Since ferryl radicals are generally good electron donors, even strongly oxidizing Mn3+can be produced from Mn2+in the presence of MnP

Fe(III) R + ROOH → FeIV = O R• + ROH (4)

FeIV = O R•+ AH2→FeIV = O R + HA• (5)

HA• + HA•→AH2+ A (6)

Where R is a protein residue, R• is the respective oxidized radical, and HA• is a substrate radical, which non enzymically decays to non- radicular products (see section below). Moreover, the efficiency of IMB and the associated degradation of TPs is also affected due to differences in electron distribution, charge density, and steric factors .

In an experiment, SW containing IMB was used to evaluate the applicability of the IMB degradation process by MnP by simulating to a real-world situation. Upon increasing TOC concentration in SW (65.67mgL-1 - typical average concentration in hospital wastewater [29]), the percentage of degradation of IMB in 8h of treatment decreased from 68% to 47%.

These results indicate that TOC has a moderate inhibitory effect on the removal of IMB during enzymatic treatment. Organic residues rich in electrons, such as activated aromatics, free amines or nitrite show considerable reactivity towards oxidants from water treatment [30,31], and could also affect the peroxy ferric complex, which affect enzyme-catalyzed reactions throughout inactivation or inhibition of the enzyme catalyst.

Oxidation of Aryl Alcohols by the MnP/Mn"/Thiol System- As shown in Table I, veratryl alcohol (I), anisyl alcohol (11), and benzyl alcohol (111) were oxidized almost quantitatively by MnP/Mn" in the presence of GSH under anaerobic con- ditions to yield the corresponding aldehydes IV, V, and VI and coupled dimers IX, X, and XI. No products were obtained when the reactions were carried out in the absence of enzyme, GSH, Mn", or H_20_2.[12] . Identical products were obtained if lactate or oxalate replaced the malonate buffer or if DTT, DTE, or Cys replaced the glutathione. Under aerobic condi- tions the same products were obtained and no veratryl alcohol ring cleavage was observed. In the presence of thiol, under anaerobic conditions, chemically prepared Mn"'-malonate was also capable of oxidizing these substituted benzyl alcohols to the corresponding alde- hyde and coupled dimer products.

The dependence of the reaction rate of the catalytic process

$2H_2O_2 + 0_2 + 2H_2O$

on the initial conditions of the reaction mixture (namely pH, catalyst concentration, temperature and ionic strength) was investigated. Pseudo-first- order conditions were maintained in all runs by the use of a large excess of H,O, over that of the manga- nese complex. Semi-logarithmic plots of the residual peroxide contents as a function of time were found to be linear up to a degree of completion of two half- lives or more. Representative sample plots obtained at -log [H'] = 9.7 and at various temperatures, are shown in. In most cases, the limiting ratio of $[H_2O_2]$/[MnY] at 75% reaction completion is greater than 22. Only in a few cases, where the dependence of the reaction rate on the catalyst concentration is studied, did this ratio approach 6-7. The influence of the concentration of the catalyst on the disproportionation reaction was determined at several pHs and temperatures.[19] In all cases, the rate is linearly proportional to the catalyst concentration. The slopes of these lines are a function of the medium pH and the temperature of the reaction mixture. At the three temperatures studied, the values of k,, are an increasing function of pH in the range of 9-O-10.3.

CONCLUSIONS

The synthesis and characterization of a new mononuclear non-heme Mn(III)peroxo species stabilized by a pentadentate N_3Py_2 ligand has been described. The species is metastable at room temperature. The Mn(III)peroxo species depicts its reactivity in aldehyde deformylation on reacting with 2-PPA. The kinetics of reactions was monitored by following the decay of the peak corresponding to Mn(III)–peroxo.

Cryogenic vibrational predissociation spectroscopy was successfully applied to identify the O - O stretching vibration in the long-lived $[Mn(tmc)O_2]^+$ reaction intermediate. The resulting spectra contain well-resolved transitions throughout the fingerprint region, most of which are derived from the tmc ligand.

I t has been demonstrated unambiguously that at least two distinct reactive intermediates, the alkyl peroxy radical, ROO,, and the Mn(IV)/alkyl peroxo adduct, MnIV(Me2EBC)(O)$(OOR)^+$, serve as epoxidizing reagents in Mn(Me2EBC)Cl^{2-}mediated oxygen-transfer reaction using alkyl hydroperoxide as the terminal oxidant. Labeling experiments using $H_2{}^{18}O$ and $^{18}O2$ provide compelling evidence .

The efficiency of MnP for degradation of imatinib in distilled water (DW) and simulated wastewater (SW) was investigated in this study. MnP enzyme was able to effectively degrade IMB, which was optimized through RSM and desirability profile where 1mgL-1 of IMB was effectively degraded at the optimal conditions of MnP = 1.12UL-1, hydrogen peroxide = 1.87mmolL-1, and Mn^{2+} = 0.755mmolL-1 within 4h. The main TPs identified in the process included a rupture in C–N bond, ring opening, and oxidative cleavage of piperazine ring, which comprised the first degradation pathway. According to the (Q) SAR analysis, most of the TPs show the development of toxicity and no biodegradability characteristics; however, a decrease in the mutagenicity potential was evident compared to the parental IMB. The results show the potential of the enzymatic method for the treatment of emerging pollutants in wastewater.

REFERENCES

1. Narulkar, D. D. *et al.* A side-on Mn(iii)-peroxo supported by a non-heme pentadentate N3Py2ligand: Synthesis, characterization and reactivity studies. *Dalt. Trans.***50**, 2824–2831 (2021).

2. Fernandez, C. A. L. Characterization and Investigation of a Binuclear Manganese (III) -Peroxo Metastable Intermediate. 1–3 (2018).

3. Hamberg, M., Su, C. & Oliw, E. Manganese lipoxygenase. Discovery of a bis-allylic hydroperoxide as product and intermediate in a lipoxygenase reaction. *J. Biol. Chem.***273**, 13080–13088 (1998).

4. Gao, Y. *et al.* Enhanced peroxymonosulfate activation via complexed Mn(II): A novel non-radical oxidation mechanism involving manganese intermediates. *Water Res.***193**, 116856 (2021).

5. Wegermann, C. A. *et al.* Synthesis, characterization and catalytic activity toward dye decolorization by manganese (II) mononuclear complexes. *Appl. Catal. A Gen.***454**, 11–20 (2013).

6. Wolk, A. B. *et al.* Isolation and characterization of a peroxo manganese (III) dioxygen reaction intermediate using cryogenic ion vibrational predissociation spectroscopy. *Int. J. Mass Spectrom.***354–355**, 33–38 (2013).

7. Zhang, R., Klaine, S., Alcantar, C. & Bratcher, F. Visible light generation of high-valent metal-oxo intermediates and mechanistic insights into catalytic oxidations. *J. Inorg. Biochem.***212**, 111246 (2020).

8. Oszajca, M., Franke, A., Brindell, M., Stochel, G. & van Eldik, R. Redox cycling in the activation of peroxides by iron porphyrin and manganese complexes. 'Catching' catalytic active intermediates. *Coord. Chem. Rev.***306**, 483–509 (2016).

9. Yin, G. *et al.* Olefin epoxidation by alkyl hydroperoxide with a novel cross-bridged cyclam manganese complex: Demonstration of oxygenation by two distinct reactive intermediates. *Inorg. Chem.***46**, 2173–2180 (2007).

10. Advanced, K. Q-. **26**, 1079–1082 (1985).

11. Lumbaque, E. C. *et al.* Degradation of imatinib mesylate by manganese peroxidase (MnP): Optimization, identification of transformation products, pathway proposal and in silico predictions. *J. Environ. Chem. Eng.***9**, 106246 (2021).

12. Vetting, M. W., Wackett, L. P., Que, L., Lipscomb, J. D. & Ohlendorf, D. H. Crystallographic Comparison of Manganese- and Iron-Dependent Homoprotocatechuate 2,3-Dioxygenases. *J. Bacteriol.* **186**, 1945–1958 (2004).

13. Wariishi, H., Valli, K. & Gold, M. H. Oxidative Cleavage of a Phenolic Diarylpropane Lignin Model Dimer by Manganese Peroxidase from Phanerochaete chrysosporium. *Biochemistry* **28**, 6017–6023 (1989).

14. Wariishi, H., Valli, K., Renganathan, V. & Gold, M. H. Thiol-mediated oxidation of nonphenolic lignin model compounds by manganese peroxidase of Phanerochaete chrysosporium. *J. Biol. Chem.* **264**, 14185–14191 (1989).

15. Nishino, H., Kamachi, H., Baba, H. & Kurosawa, K. Manganese(III)-Mediated Carbon-Carbon Bond Formation in the Reaction. 3551–3557 (1992).

16. Saisaha, P., de Boer, J. W. & Browne, W. R. Mechanisms in manganese catalysed oxidation of alkenes with H2O2. *Chem. Soc. Rev.* **42**, 2059–2074 (2013).

17. Frostin-rio, M., Pujol, D., Bied-charreton, C. & Fauvet, M. P.-. 6""b \ / ' 0. 1971–1979 (1984).

18. Rizkalla, E. N., Anis, S. S. & Khalil, L. H. The kinetics and mechanisms of the catalysed decomposition of hydrogen peroxide by ethylenediaminetetra(methylenephosphonato) complex of manganese(II). *Polyhedron* **6**, 403–409 (1987).

19. Wang, L., Ma, Y., Jiang, Y., Lv, L. & Li, Z. A Mn-catalyzed remote C(sp3)-H bond peroxidation triggered by radical trifluoromethylation of unactivated alkenes. *Chem. Commun.* **57**, 7846–7849 (2021).

20. Seo, M. S. *et al.* [Mn(tmc)(O2)]+: A Side-On Peroxido Manganese(III) Complex Bearing a Non-Heme Ligand. *Angew. Chemie* **119**, 381–384 (2007).

21. Annaraj, J. *et al.* Structural characterization and remarkable axial ligand effect on the nucleophilic reactivity of a nonheme manganese(III)-peroxo complex. *Angew. Chemie - Int. Ed.* **48**, 4150–4153 (2009).